Multi-scale Dynamics, Control, and Simulation of Granular Spacecraft[1]

Marco B. Quadrelli[1], Scott Basinger[1], Grover Swartzlander[2]

[1] *Jet Propulsion Laboratory, California Institute of Technology, 4800 Oak Grove Drive, Pasadena, CA 91109-8099, Mail Stop 198-219, Marco.B.Quadrelli@jpl.nasa.gov, Scott.Basinger@jpl.nasa.gov*

[2] *Center for Imaging Science and Physics Dept., Rochester Institute of Technology, 54 Lomb Memorial Drive, Rochester, NY 14623, grovers@mail.rit.edu*

Abstract

In this paper, we present some ideas regarding the modeling, dynamics and control aspects of *granular spacecraft*. Granular spacecraft are complex multibody systems composed of a spatially disordered distribution of a large number of elements, for instance a cloud of grains in orbit. An example of application is a spaceborne observatory for exoplanet imaging, where the primary aperture is a cloud instead of a monolithic aperture. A model is proposed of the multi-scale dynamics of the grains and cloud in orbit, as well as a control approach for cloud shape maintenance and alignment, and preliminary simulation studies are carried out for the representative imaging system.

Keywords: *multibody dynamics, spacecraft, granular media, distributed systems*

1 Introduction

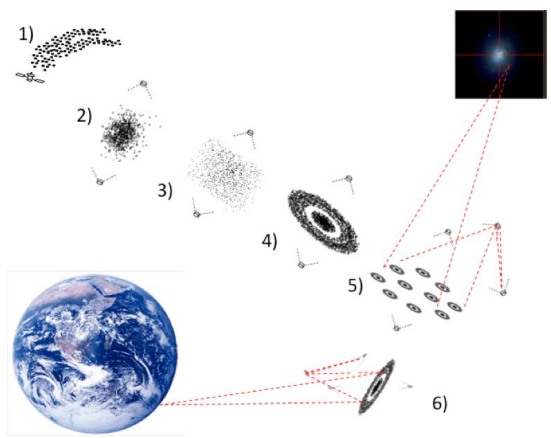

Figure 1. Scenario of application of a granular spacecraft.

The useful engineering properties of a cloud of granular matter in space are virtually unknown. Granular matter is considered to be the 5th state of matter (after solid, liquid, gaseous, and plasma) by virtue of its peculiar response characteristics (cohesiveness, fluid behavior, compactification, phase transformation capability, and others) [6]. However, it is a fact that the dynamics, controllable properties, and consequent benefits of engineering and manipulating granular matter such as dust grains, powders, and granular spacecraft is poorly known to the space exploration community.

In this paper, we present some ideas regarding the modeling, dynamics and control aspects of *granular spacecraft*. Granular spacecraft are complex multibody systems composed of a spatially disordered distribution of a large number of elements, for instance a cloud of N grains in orbit, with $N>10^3$. We address the modeling and autonomous operation of a distributed assembly (the cloud) of large numbers of highly miniaturized space-borne elements (the grains). A granular spacecraft can be defined as a collection of a large number of space-borne elements (in the 1000s) designed and controlled such that a desirable collective behavior emerges, either from the interactions among neighboring grains, and/or between the grains and the environment. The ultimate objective would be to study the behavior of the single grains and of large ensembles of grains in orbit and to identify ways to guide and control the shape of a cloud composed of these grains so that it can perform a useful function in space, for instance, as an element of an optical imaging system for astrophysical applications. This concept, in which the aperture does not need to be continuous and monolithic, would increase the aperture size several times compared to large NASA space-borne observatories currently envisioned such as ATLAST, allowing for a true Terrestrial Planet Imager that would be able to resolve exo-planet details and do meaningful spectroscopy on distant worlds. To accomplish this goal, we need to investigate the conditions to

[1] This research was carried out at the Jet Propulsion Laboratory, California Institute of Technology, under a contract with the National Aeronautic and Space Administration. © 2013. All rights reserved.

manipulate and maintain the shape of an orbiting cloud of dust-like matter so that it can function as an ultra-lightweight surface with useful and adaptable electromagnetic characteristics. Consider the following scenario, shown in Figure 1: 1) the cloud is first released; 2) it is contained by laser pressure to avoid dissipation and disruption by gravitational tidal forces, 3) it is shaped by optical manipulation into a two-dimensional object (coarse control), and 4) ultimately into a surface with imaging characteristics (fine control). The cloud shape has to be maintained against orbital disturbances by continuous figure control, also achieved optically. Applying differential light pressure retargets the entire cloud, so that a change of the optical axis can be induced. Selected parts of the cloud are reshaped when required for wavefront control, thus enabling higher quality optics. The entire imaging system is now in full operation, as 5) a multilens system searching for exo-planets, or 6) as a radio receiver engaged in remote sensing investigations. The potential advantages of the granular spacecraft concept are that: a) it can result in an ultra-lightweight system, made of very simple, very low cost, units; b) it can be very big: the cloud can distribute itself to kilometer scales, without the need to fill the aperture; c) the cloud is easy to package, transport and deploy; d) it is reconfigurable, and can be retargeted and repointed with non-mechanical means; e) the cloud is a highly fault-tolerant system with very low vulnerability to impacts. Other potential advantages offered by the cloud properties as optical system involve possible combination of properties (combined transmit/receive), variable focal length, combined refractive and reflective lens designs, and hyper-spectral imaging.

The study of granular spacecraft involves different disciplines, some of which are outlined in Figure 2: gravito-electrodynamics, optics, laser-matter interaction, disordered and distributed systems, multi-scale simulation, formation-flying, granular media, and plasma physics, among others. Because it is such a complex problem, this paper only scratches the surface and proposes a systemic view by first making some modeling considerations in section 2, discussing the physics of the problem in Section 3, a representative example in Section 4 and its numerical simulation in Section 5. A discussion of preliminary numerical results concludes the paper.

2 Modeling considerations

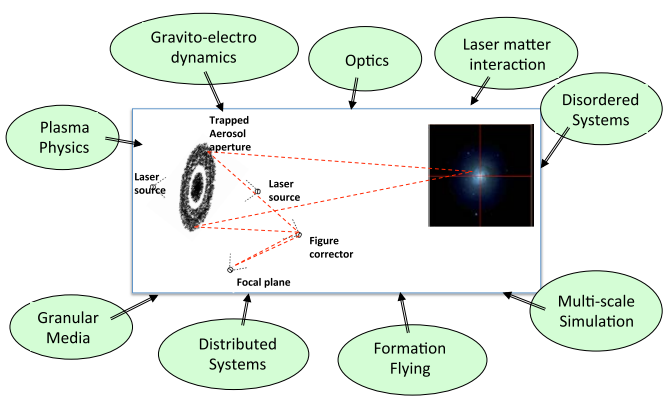

Figure 2. Multi-disciplinary elements of problem.

Modeling of granular spacecraft is more challenging than modeling of conventional space-borne vehicles because we are faced with a probabilistic vehicle composed of a large number of physically disconnected vehicles. First, different scales of motion occur simultaneously in a cloud: translations and rotations of the cloud as a whole (*macro-dynamics*), relative rotation and translation of one cloud member with respect to another (*meso-dynamics*), and individual cloud member dynamics (*micro-dynamics*). A major challenge is to incorporate these modes of motion into a reduced order model. There exist at least two time scales, as well as at least two space scales, in the description of the dynamics of a cloud. The dynamics of an individual vehicle begin to emerge when the time scale of a stimulus (internal or external to the cloud) is smaller than the time scale representative of the cloud dynamics itself. Similarly, in the opposite case the cloud behavior as an integrated unit is predominant. This behavior affects the stability of the system as cloud cohesiveness depends on the internal space and time scales. Furthermore, these effects become more complicated and nonlinear when the cloud undergoes large reconfigurations, both in relative translation and in attitude with respect to a reference configuration. These systems also display both a *local* and a *non-local* aspect. The local aspect pertains to the near-collocation represented by a sensor and an actuator located on the cloud. The non-local aspect appears when a sensor located on one end of the cloud feels the effect of an actuator mounted on another one at a different location. Second, the control design needs to be tolerant of the system complexity, of the system architecture (centralized vs. decentralized large scale system control) as well as robust to un-modelled dynamics and noise sources. Optimized sensor locations and robust dynamics estimation schemes are required to achieve full knowledge of the states of the system within a significant cluster of individual grains. Additionally, information processing on a granular spacecraft is inherently distributed by nature. Modeling of a cloud cannot dispense with the need to appropriately model the latencies and bandwidth limitations associated with inter-cloud communications. Single vehicle applications are immune to such considerations. Simulation of a cloud must also address a large range of spatial and temporal scales, which intrinsically make the problem numerically stiff in nature. It is in effect a multiple-scale problem, a solution to which will require a new class of numerical algorithms with special demands on accuracy, stability, and provision for coexisting multiple time scales. Table 1 shows a comparison of

various requirements for simulation of single spacecraft vs. granular spacecraft, indicating the high degree of complexity that needs to be taken into consideration.

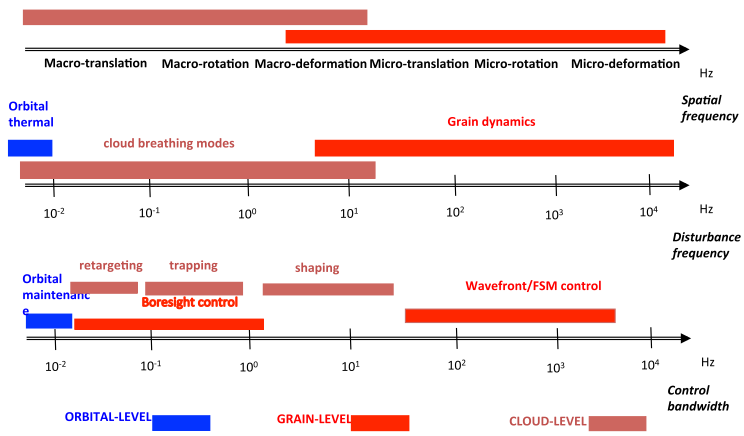

Figure 3. Spatial, temporal, and control scales involved in the granular spacecraft problem.

Three spatial and temporal domains can be identified: a) micro, at the scale of the individual vehicle; b) meso, at the scale of a cluster of vehicles within the cloud; and c) macro, at the scale of a very large number of vehicles. Figure 3 shows the different spatial and temporal scales involved in the system. While the micro-, meso-, macro-scales affect the spatial frequency distribution, depending on the disturbance frequency various parts of the system are excited differently. Furthermore, to be useful as an engineering system, the various control bandwidths of interest must be considered at the orbital level, grain level, and cloud level.

From the point of view of modeling the system, two main problems are identified. First, the Direct Problem, in which given the individual cloud elements, interconnectivity dictated by communication constraints, and local potential functions describing the interaction (or collision avoidance constraint) between adjacent elements, predict the global motion of the cloud and control it according to an optimality criterion. Second, the Inverse Problem: given a desired trajectory for the cloud, determine the interconnectivity and local potential functions between adjacent elements of the cloud that result in the desired motion. In this paper we deal only with the Direct problem.

By means of micro-continuum field theory ([2], [5], [12]), we can unify the deformation and dynamics modalities of a cloud. We use continuum mechanic constructs for this analysis. Each individual grain is endowed with a position vector, a rotation tensor, and a deformation gradient tensor, in the spirit of micromorphic kinematics. This means that each individual grain is capable of changing its configuration in response to stimuli originated either from the exterior of the cloud or within the cloud itself. The cloud is therefore treated as a continuum at the macroscopic level, with added extra structure at the micro-continuum, or particle, level. A set of balance laws for the cloud can then be derived, assuming invariance of the cloud energy functional to translations and rigid rotations. These balance laws include the conservation of the cloud mass, the balance of cloud linear momentum, the balance of macroscopic cloud angular momentum and of particle angular momentum, the cloud entropy inequality, and the boundary conditions at the boundary of the cloud. The description of the internal constitution of the cloud, i.e. the constitutive relation between internal reconfiguration kinematic variables (strains) and internal reconfiguration momenta, completes the mechanical description of the cloud. The internal reconfiguration momenta represent the generalized inertia and the generalized stresses that the individual grain experiences when a reconfiguration is taking place. The constitutive functional includes memory dependent terms and nonlocality in the cloud response [17]. That this must be included stems from the fact that the behavior of the cloud can be influenced both at the system level and at the individual grain level. Therefore, two time scales enter the picture, as well as two space scales. The individual grain dynamics begins to emerge when $(\lambda/L)\approx 1$, where λ is the time (or space) scale of the stimuli internal or external to the cloud, whereas L is a time (or space) scale representative of the cloud itself. When $(\lambda/L)<<1$, the individual grain behavior is predominant, and when $(\lambda/L)>>1$, the cloud behavior as a unit is predominant. The spatial nonlocality occurs since one grain may respond to stimuli from another grain located far away from it in the cloud, and it occurs also at a global level, since each grain may respond to stimuli of the cloud as a unit. This multilevel behavior is reflected in the nonlocal constitutive functional. Memory dependence, also known as time nonlocality, enters the constitutive functional through time dependence of the current instant from previous instants. Since both the target location knowledge and the physical grain (and sensor) locations are stochastic in nature, we use the concept of random fields to set up an equivalent boundary value problem in the time domain where the

Table 1. Comparison of requirements for simulation of single spacecraft vs. granular spacecraft.

	Single SC	cloud
Propagation model	Serial	Distributed/parallel
Workspace volume	Small	Very large
Input data structure	Small	Very large
Output data structure	Small	Very large
Significant digits	Many	few
Spatial scales of motion	Orbital/attitude/flex	Orbital/micro/meso/macro
Temporal scales of motion	Orbital/attitude/flex	Orbital/micro/meso/macro
Disturbance frequency	Orbital period	Orbital/micro/macro
Controller bandwidth	ACS+DV	ACS+DV+reconfiguration +containment
Computation on GPU	Not needed	Recommended

coefficients of the differential operator are random processes. A description of the cloud dynamics within the spatial domain Ω can then be cast as a boundary value problem ([7], [8]) as

$$[B(x,t) + G(x,t;\omega)]\, u(x,t;\omega) = f(x,t;\omega) \tag{1}$$

together with the appropriate boundary conditions at the boundary of Ω, where x is the spatial scale, t is the temporal scale, ω is a random fluctuation, B is the deterministic operator describing the dynamics, G is the stochastic part whose coefficients are zero-mean random processes, and f is the vector of exogenous and control inputs. It is clear that, depending on the connectivity between the elements of the cloud, the B and G operators may be local or nonlocal operators derived from variational principles expressed in their weak form. This approach ensures a robust mathematical formulation since the stochastic nature of the states is reflected in the stochastic nature of the differential operators.

3 Cloud Physics

To address the engineering applications, we need to have insight on physics of disorder systems and the dominant forces that perturb the cloud. Related background can be found in refs [13], [19], [23]. Cloud gravito-electrodynamics leads to self-organization: for a cloud of particles released from an orbiting vehicle, the diffusion characteristics are important, as well as the tendency to form natural ring-like structures governed by the local gravity gradients, solar pressure, and radiation properties of each individual grain. The electrodynamic Lorentz coupling in LEO-GEO provides high degree of structural coherence which can be exploited in applicaitons. Once illuminated, the diffraction pattern from a disordered assembly leads to a strong focusing potential: the intensity of the signal is more collimated when the distribution of apertures is randomized, the separation between apertures increases, and the number of apertures increases. Focusing is achieved by modulating the phase of the distributed radiators so as to obtain a conic phase surface, and this leads naturally to the shaping a cloud in the form of a lens. In space, the cloud behavior depends on the dynamic balance of different force fields: Laser light pressure, as light can induce motion; Solar illumination radiation pressure, which carries momentum; Gravitational forces and gradients, resulting in orbital and tidal effects; Electrostatic Coulomb or dielectrophoretic forces, since the grains are charged; Electromagnetic Lorentz forces resulting from the interaction with local magnetic field; Cloud self-gravity caused by the cloud being an extended body; Poynting-Robertson drag, in which grains tends to spiral down towards the Sun; and Yarkovstky (YORP) effect, caused by the anisotropic emission of thermal photons, which carry momentum. In the next sections, we describe the gravito-electrodynamics coupling, and the opto-mechanical interaction.

3.1 Cloud Gravito-electrodynamics

To gain some insight into the physics of the problem, we can for the time being consider the dynamics of one grain and of a collection of grains separately. The equation of motion of one grain around planet rotating at Ω_p:

$$\ddot{\mathbf{r}} = -\frac{\mu \mathbf{r}}{m|\mathbf{r}|^3} + \frac{Q(r)}{mc}\left[\dot{\mathbf{r}} \times \mathbf{B}(\mathbf{r}) - (\Omega_p \times \mathbf{r}) \times \mathbf{B}(\mathbf{r})\right] + \mathbf{F}(\mathbf{r}) \cdot \tag{1}$$

from which the resulting natural frequencies are

$$\Omega = \frac{\Omega_B}{2}\left\{1 \pm \left[1 + 4\left(\frac{\Omega_K^2}{\Omega_B^2} - \frac{\Omega_p}{\Omega_B}\right)\right]^{1/2}\right\}. \tag{2}$$

where Ω_B is the plasma gyro-frequency, Ω_p is the planet rotation rate, and Ω_K is the Keplerian frequency, indicating that gravity, electromagnetic fields are coupled and interact with local plasma. For a cloud of particles released from an orbiting vehicle, the diffusion characteristics are important, as well as the tendency to form natural ring-like structures governed by the local gravity gradients, solar pressure, and radiation properties of each individual grain. As a system the orbital mechanics of a cloud can be modeled by the following equations:

$$\ddot{R}_0 - \dot{v}^2 R_0 = -\frac{\mu}{R_0^2}\left[1 + \frac{3}{2mR_0^2}\left(trace(J) - 3J_1 \sin^2\alpha - 3J_3\cos^2\alpha\right)\right] - \frac{f}{m}\cos\left(\alpha+\theta\right)$$

$$\ddot{v} + 2\frac{\dot{R}_0}{R_0}\dot{v} = -\frac{3\mu}{mR_0^5}\left(J_3 - J_1\right)\sin\alpha\cos\alpha - \frac{f}{mR_0}\sin\left(\alpha+\theta\right) \tag{3}$$

$$\ddot{\alpha} - \ddot{v} = \frac{3\mu}{R_0^3}\frac{\left(J_3 - J_1\right)}{J_2}\sin\alpha\cos\alpha + \frac{f}{J_2}\left(d_3\sin\theta - d_1\cos\theta\right)$$

These equations apply to an extended cloud of total mass m and moments of inertia J_1, J_2, J_3 in the baricentric frame. The equations of motion are nonlinear and non-homogeneous and apply to any type of orbit. The attitude dynamics and the orbital dynamics are, indeed, coupled through the pitch angle α, which is not necessarily small, and through the true anomaly v. When the orbit is circular, the cloud attitude dynamics is uncoupled from the orbital dynamics. The overallthrust direction (θ) and magnitude (f) affect both the orbital and attitude dynamics. The gravity gradient effect (represented by the terms in $sin\alpha$ and $cos\alpha$) appears in all the equations. This state coupling has not yet been investigated in the literature. Now, let us consider the local vertical-local horizontal (LVLH) frame F_o, and let's look at the point located at $\rho = \begin{pmatrix} x & y & z \end{pmatrix} F_o$ from the origin of the moving coordinate system. Its relative acceleration in F_o *is:*

$$\ddot{\rho}_i = -\dot{\mathrm{V}}_0 - \left(\dot{\Omega}^\times + \Omega^\times\Omega^\times\right)\rho_i - 2\Omega^\times\dot{\rho}_i + a_{\mathbf{i}}(r_i, \dot{r}_i, t) \tag{4}$$

Then its gradient tensor can be computed in matrix form as:

$$\Gamma_{ij} = \frac{\partial\ddot{\rho}_i}{\partial\rho_j} = -\left(\dot{\Omega}^\times + \Omega^\times\Omega^\times\right) + \frac{\partial}{\partial\rho_j}\left[a_{\mathbf{i}}(r_i, \dot{r}_i, t)\right] = -\left(\dot{\Omega}^\times + \Omega^\times\Omega^\times\right) + \frac{\partial a_i}{\partial r_i}\bullet\frac{\partial r_i}{\partial\rho_j} + \frac{\partial a_i}{\partial\dot{r}_i}\bullet\frac{\partial\dot{r}_i}{\partial\rho_j} \tag{5}$$

Similarly, its gyroscopic tensor can be computed in matrix form as:

$$\Upsilon_{ij} = \frac{\partial\ddot{\rho}_i}{\partial\dot{\rho}_j} = -2\Omega^\times + \frac{\partial}{\partial\dot{\rho}_j}\left[a_{\mathbf{i}}(r_i, \dot{r}_i, t)\right] = -2\Omega^\times + \frac{\partial a_i}{\partial\dot{r}_i}\bullet\frac{\partial\dot{r}_i}{\partial\dot{\rho}_j} \tag{6}$$

Taking the instantaneous orbit of 0 as reference, we can now look at the motion with respect to the moving origin, still nonlinear in the kinematics, by expanding the perturbation force in Taylor series about the reference configuration. Consequently, the TANGENT equations of motion can be written as:

$$m_i 1_3 \ddot{\rho}_i + [\Upsilon]_i\dot{\rho}_i + [\Gamma]_i\rho_i = -\dot{\mathrm{V}}_0 + C_{oi}\left[\frac{f_{\mathbf{i}}(\rho_i, \dot{\rho}_i, \rho_j, \dot{\rho}_j, ...)}{m_i}\right]_0 + H.O.T. \tag{7}$$

As an example, consider a one-dimensional cloud. Consider the simple case of circular orbit with $R_0 = \begin{pmatrix} 0 & 0 & R_0 \end{pmatrix} F_o$ and $\Omega = \begin{pmatrix} \omega_0 & 0 & 0 \end{pmatrix} F_o$, for which the gravitational gradient tensor becomes:

$$\Gamma_{ij} = \frac{\partial\ddot{\rho}_i}{\partial\rho_j} = -\left(\dot{\Omega}^\times + \Omega^\times\Omega^\times\right) - \frac{\mu}{\left|R_0\right|^3}\frac{\partial}{\partial\rho_j}\left[R_0 + \rho_i - 3\frac{\left(R_0\bullet\rho_i\right)}{\left|R_0\right|^2}R_0\right] \tag{8}$$

Then, the components of the gravitational gradient tensor are $\Gamma_{11} = -\omega_0^2$, $\Gamma_{33} = 3\omega_0^2$, which imply that the motion along x (along normal to orbital plane) is compressive, the motion along y (along velocity vector) experience no force, and the motion along z (along local vertical) is tensile.

3.2 Opto-mechanical Interactions

A spherical particle in the presence of light will experience both a scattering force in the direction of the beam axis, which is proportional to the irradiance, and a gradient force that may be expressed as F_{grad}=-(1/2)α(gradE)^2, where α is the polarizability of the particle [1], [3], . The gradient force is the direction of the beam axis is negligible unless the beam is tightly focus. Beam shaping of a cloud of particles is possible by molding the cloud in with the gradient force, say in the x-y plane, and by further molding the cloud in the z-direction by the combined optical scattering force and gravitational forces arising from the orbital dynamics (tidal forces). At the moment of release the velocity distribution of the cloud may be represented by a probability distribution such as the Maxwell-Boltzmann distribution. Without intervention, the cloud will diffuse to a rarified state where the particles move ballistically. The gradient force required

to "freeze" the distribution in the x-y plane must then be of the order of $F_{grad}=m\sqrt{(2k_BT/m)}/\Delta t$, where Δt is the beam exposure time, T is the temperature, m is the particle mass, and k_B is Boltzmann's constant. The expansion of a rarefied gas cloud in vacuum expands as $\exp(-\tau^2/t^2)$ where $\tau^2 = mR^2/2k_BT$, and R is a diffusion length [18]. The required irradiance, I, may therefore be estimated as $I = 4k_BT/\alpha\eta$, where η=377 [Ω] is the impedance of free space, and $\alpha = 4\pi\varepsilon_0 a^3$, where a is the radius of a grain, and ε_0=8.9E-12 [F/m]. For a radius of 1 micron, the irradiance becomes of the order of 13 kW/m^2, a CW laser power level which is within the range of commercial lasers in the visible band, including Nd:YAG laser at 532 nm. Although the radiation pressure force on a macroscopic body is weak, a few milliwatts of focused laser power are sufficient to achieve a force in the piconewton range. For a micron-sized body, the laser power is in the nanowatt range. Figure 4 depicts the estimates of orbital forces and optical power involved in cloud trapping as a function of grain diameter.

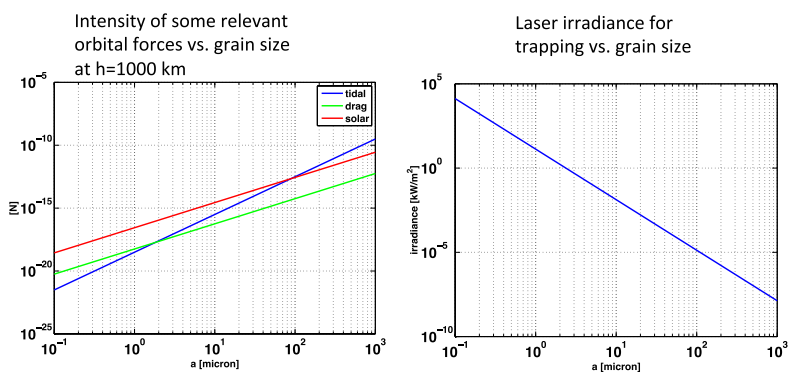

Figure 4. Estimates of orbital forces and optical power involved in cloud trapping.

4 Granular spacecraft modeling and simulation

Two simulations are currently being developed for systems engineering evaluations of proof-of-concept: one simulation of dynamics and control of "virtual truss" model of imaging system in formation, and one simulation of gravito-electrodynamics and control of cloud of grains subject to environmental disturbances and field control (electromagnetic, optical, gravitational). The focus of this paper is the second one.

The cloud simulation software is based on building a model of a large number of identical grains. This simulation environment allows trade studies for autonomy selection, trade studies for orbit selection for different applications, testing of autonomy algorithms at grain level and cloud level, development and testing of modeling and propagation algorithms. The grain model involves fully nonlinear dynamics with sensors/actuator models. One level of control for cloud shape maintenance, drift control, and another level of control is for cloud attitude stabilization. The cloud model involves an equivalent rigid body with coupled micro/macro motion. The disturbances modeled are Gravity, Third-Body, Drag, solar, EM field, thermal balance.

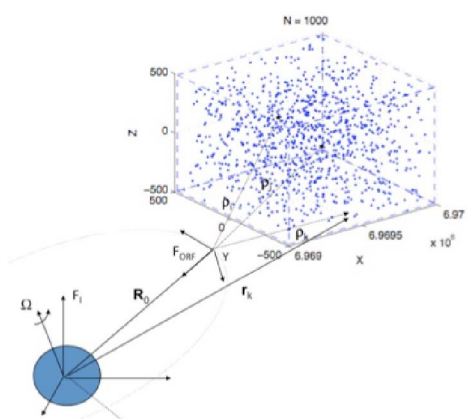

Figure 5. Orbital parameters of cloud in orbit.

The assumptions we used to model the dynamics are as follows: 1) The inertial frame is fixed at Earth's center. 2) The orbiting Frame ORF follows Keplerian orbit. 3) the cloud system dynamics is referred to ORF. 4) the attitude of each grain uses the principal body frame as body fixed frame. 5) the atmosphere is assumed to be rigidly rotating with the Earth. Regarding the grains forming the cloud: 1) each grain is modeled as a rigid body; 2) a simple attitude estimator provides attitude estimates, 3) a simple guidance logic commands the position and attitude of each grain, 4) a simple local feedback controller based on PD control of local states is used to stabilize the attitude of the vehicle. Regarding the cloud: 1) the cloud as a whole is modeled as an equivalent rigid body in orbit, and 2) an associated graph establishes grain connectivity and enables coupling between modes of motion at the micro and macro scales; 3) a simple guidance and estimation logic is modeled to estimate and command the attitude of this equivalent rigid body; 4) a cloud shape maintenance controller is based on the dynamics of a stable virtual truss in the orbiting frame. Regarding the environmental perturbations acting on the cloud: 1) a non-spherical gravity field including J0 (Earth's spherical field) zonal component, J2 (Earth's oblateness) and J3 zonal components is implemented; 2) atmospheric drag is modeled with an exponential model; 3) solar pressure is modeled assuming the Sun is inertially fixed; and 4) the Earth's

magnetic field is model using an equivalent dipole model. The equations of motion are written in a referential system with respect to the origin of the orbiting frame and the state is propagated forward in time using an incremental predictor-corrector scheme.

Figure 5, shows the kinematic parameters of a 1000 element cloud in orbit. The motion of the system is described with respect to a local vertical-local horizontal (LV-LH) orbiting reference frame (x,y,z)=F_{ORF} of origin O_{ORF} which rotates with mean motion Ω and orbital semi-major axis R_0. The orbital geometry at the initial time is defined in terms of its six orbital elements, and the orbital dynamics equation for point O_{ORF} is propagated forward in time under the influence of the gravitational field of the primary and other external perturbations, described below. The origin of this frame coincides with the initial position of the center of mass of the system, and the coordinate axes are z along the local vertical, x toward the flight direction, and y in the orbit normal direction. The inertial reference frame (X,Y,Z)=F_I is geocentric inertial for LEO (X points toward the vernal equinox, Z toward the North Pole, and Y completes the right handed reference frame), and heliocentric inertial for other applications. The orbit of the origin of F_{ORF} is defined by the six orbital elements a (semimajor axis), e (eccentricity), i (inclination), Ω_L (longitude of ascending node), w (argument of perigee), ν (true anomaly), and time of passage through periapsis. From Figure 1, the position vector of a generic grain with respect to O_{ORF} is denoted by $\boldsymbol{\rho}_i$, and we have $\mathbf{r}_i=\mathbf{R}_0+\boldsymbol{\rho}_i$. We define the state vector as

$$\mathbf{X}=\left(\mathbf{r}_E,\dot{\mathbf{r}}_E,\mathbf{R}_0,\dot{\mathbf{R}}_0,\ldots\rho_i,\mathbf{q}_i,\dot{\rho}_i,\omega_i,\mathbf{R}_s,\dot{\mathbf{R}}_s,\rho_s,\dot{\rho}_s,\mathbf{q}_s,\omega_s\right) \tag{9}$$

where $\mathbf{q}_i$ and $\boldsymbol{\omega}_i$ represent the quaternion and angular velocity vector of the i-th grain with respect to F_I. The translation and rotation kinematics at the grain level are:

$$\text{grain}\begin{cases}\mathbf{V}_0=\dot{\mathbf{R}}_0\\ \mathbf{v}_i=\dot{\rho}_i\\ \dot{\mathbf{R}}_{bi}=-\omega^{\times}\mathbf{R}_{bi}\end{cases}\qquad \text{cloud}\begin{cases}\mathbf{V}_s=\dot{\mathbf{R}}_s\\ \mathbf{v}_s=\dot{\rho}_s\\ \dot{\mathbf{C}}_{si}=-\omega_s^{\times}\mathbf{C}_{si}\end{cases} \tag{10}$$

The angular momentum balance is:

$$\begin{aligned}&\text{grain}\quad \mathbf{J}_i\dot{\omega}_i+\omega_i^{\times}\mathbf{J}_i\omega_i=\sum_{j=1}^{Npert}\tau_j\\ &\text{cloud}\quad \mathbf{J}_s\dot{\omega}_s+\omega_s^{\times}\mathbf{J}_s\omega_s=\tau_s\end{aligned} \tag{11}$$

and the linear momentum balance is:

$$\text{grain}\begin{cases}\dot{\mathbf{V}}_0=-\mu_E\dfrac{\mathbf{R}_0}{|R_0|^3}+\dfrac{\sum_{j=1}^{Npert}\mathbf{f}_j}{m_{total}}\\ \ddot{\rho}_i=-\dot{\mathbf{V}}_0-\dot{\boldsymbol{\Omega}}^{\times}\rho_i+\boldsymbol{\Omega}^{\times}\boldsymbol{\Omega}^{\times}\rho_i-2\boldsymbol{\Omega}^{\times}\dot{\rho}_i+\mathrm{A}_i\ddot{\mathbf{r}}_i\\ \ddot{\mathbf{r}}_i=-\mu_E\dfrac{\mathbf{r}_i}{|\mathbf{r}_i|^3}+\dfrac{(\mathbf{f}_a+\mathbf{f}_e)_i}{m_i}\end{cases}\qquad \text{cloud}\begin{cases}\dot{\mathbf{V}}_s=-\mu_E\dfrac{\mathbf{R}_s}{|R_s|^3}+\dfrac{(\mathbf{f}_{J2}+\mathbf{f}_{J3})_s}{m_s}\\ \ddot{\rho}_s=-\dot{\mathbf{V}}_s-\dot{\boldsymbol{\Omega}}^{\times}\rho_s+\boldsymbol{\Omega}^{\times}\boldsymbol{\Omega}^{\times}\rho_s-2\boldsymbol{\Omega}^{\times}\dot{\rho}_s+C_{si}\dfrac{\mathbf{f}_s}{m_s}\end{cases} \tag{12}$$

where: A_i= rotation matrix of i-th body frame wrt. Inertial; R_0= orbital radius vector to origin of ORF; Ω = orbital rate; C_{si}= rotation matrix of cloud body frame wrt. Inertial; $f_{a,e}$ = actuation + external forces (gravity, aerodynamics, magnetic, solar); $m_{i,s}$ = grain/cloud mass; $w_{i,s}$ = body, cloud angular rate; $\tau_{a,e}$ = actuation + external torques; $J_{i,s}$ = grain/cloud moment of inertia.

5 Application to Control of a Representative Optical Imaging System

Resolution and aperture sizes for astrophysical optical systems are ever increasing in demand [14], [16]. With near-term plans to build 30 meter ground-based telescopes for astronomy, the demand for higher resolution optics in space continues to grow not only for exo-planet detection, but also for earth-based science, including hyper-spectral imaging and for monitoring of the oceans and land masses (e.g. seismic monitoring). ATLAST, still several decades away, is the largest practical space telescope designed using state-of-the-art light-weight segmented mirror technology: it may have an aperture up to 18 m. The aperture formed by the granular spacecraft cloud does not need to be continuous. Used interferometrically, for example, as in a Golay array [4], imagery can be synthesized over an enormous scale. As part of our investigation, we have considered refractive, reflective and holographic systems and outlined optical correction and collection systems. In addition to forming a single monolithic optical element with the cloud, we also considered forming smaller self-coherent patches, similar to segments in a segmented aperture, but not required to be phased with respect to each other. The "segments" can be continuous or separated by large amounts to form a sparse

array. A corrector is then used to compensate for phase differences between each "segment". A Fizeau interferometer is a straightforward corrector for a reflective system. A more advance corrector would be a multiple aperture system utilizing multi-scale lens design, as described by [4]. The multi-scale lens design has the additional benefit of an increased field of view of the optical system and will allow for less movement of the entire collection of sub-apertures when changing the line of sight of the system.

An optical imaging system design has been selected as the best candidate architecture for a space system involving a cloud. The concept design is shown in Figure 6. The sequence of optics is as follows: the starlight is focused by granular spacecraft optic "patch", creating a spherical wavefront. Light from all patches converges at an intermediate focus, which has an image-plane coded aperture. The light then reflects off secondary mirror (Gregorian) and the light from each patch is collimated. Each beam goes to a separate adaptive optics system. A fast steering mirror and a deformable mirror correct pointing and low to mid-spatial frequency aberrations. An optical delay line is used to correct phasing difference between the patches and allow for Fourier transform spectroscopy. A beam-splitter is included to allow some of the light to go to a Shack-Hartmann sensor to measure aberrations in the system. For this system, the selected approach for cloud management/sensing/control is multistage, with an outer stage for formation stabilization, and an inner stage for telescope wavefront sensing and correction, relegating fine adaptive optics to a deformable/fast steering mirror stage in the optical bench. The system's relative range/bearing sensing and metrology is based on virtual telescope formation flying, in which distributed relative sensing is accomplished using Ka-Band transceivers/patch antennas, and a centralized laser metrology system, relying on a single laser source on the main light-collecting spacecraft, while single reflecting target are on other free-flying elements except granular spacecraft.

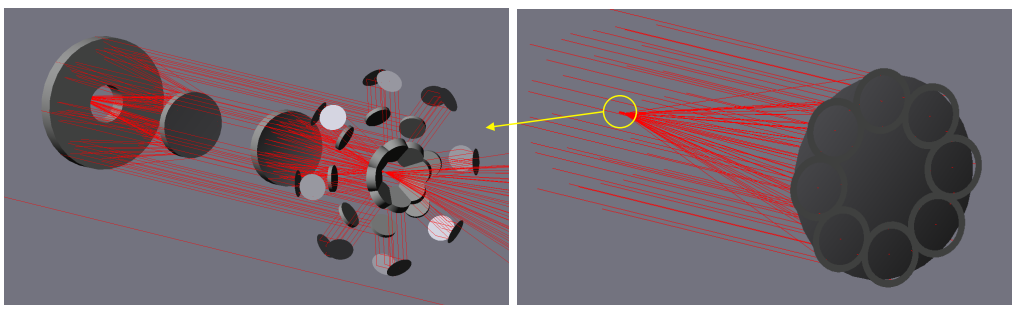

Figure 6. Reflective imaging system concept design with 8 cloud patches forming the aperture.

The cloud sensing approach is based on imaging/laser scanning, relying on custom or commercial stereo vision or laser scanning systems which can create precise 3-D model of complex objects. The approach for cloud control is multistage, based on laser cooling, and involves three levels: a) Trapping ("corralling") through gradient forces to provide containment against cloud diffusion due to thermal, radiation, and gravity and cloud cooling; b) shaping/alignment through laser pressure, to change amorphous cloud into disk or rectangular carpet; and c) alignment of grains to wavefront direction, which implements wavefront/boresight control through adaptive optics in order to maintain optical figure. Related work is presented in [2], [10], [11], [14]. For any size/shape particle, the electromagnetic energy is minimized when the particle is in the brightest region of the laser beam, and this is the basis for light-induced control. Corralling assumes mechanically releasing the cloud with low ejection velocities, then applying 3-axis laser illumination to corral the cloud via optical gradient forces. The cooling approach can be achieved by means of gradient forces, which involves rotating the linear polarization direction of the control laser at the rocking frequency. This effectively freezes the oscillations in a rotating reference frame. By adiabatically slowing the rotation of the polarization axis, some population of particles can be made to assume the same orientation, e.g., with the flat mirrored side of the rod facing the center of curvature. Cloud shaping is carried out via raster scanning of the beam across granular patch. An optimization is needed of the time dependent beam power and beam velocity to capture the most particles, and will be subject of future work. Grain alignment for phase coherence is achieved by applying linearly polarized control laser to orient particles along dominant polarization axis (long axis of rod), so that the particles will rock under the influence of polarization torque and radiation pressure torque.

A representative cloud with varying number of grains is simulated to identify the limitations in computation time as the number of grains grows. We can derive a control law to track a desired surface in the ORF (equivalently to maintain a reference cloud shape) as follows [15], [21], [22]. Define the tracking error $e_Z = q(x,y) - q_d(x,y)$, where $q_d(x,y)$ are the desired surface, and q(x,y) the current position of the grain belonging to that surface with respect to the origin of ORF. By imposing an exponentially stable error dynamics in the form $\ddot{e}_Z + 2\zeta_Z \omega_Z \dot{e}_Z + \omega_Z^2 e_Z = 0$, we can make sure the error *e* is driven to zero. Therefore, using the equations of motion expressed in ORF coordinates, the feedback-feedforward control law with components in ORF becomes:

$$u = -f_{pert} + f_{gyro} + m\ddot{q}_{des} - K_d\dot{e} - K_p e\,. \tag{13}$$

where f_{pert} is the resultant of the gravitational forces on the grain, f_{gyro} are the Coriolis and centrifugal forces acting on the grain, Kd is a derivative gain, and Kp is a proportional gain. Both f_{pert} and f_{gyro} can be modeled, act on a time scale which is very long, and can be canceled out by the feed-forward control scheme. These control forces are applied by the laser scanning system, coupling mechanically with the grains via opto-mechanical interaction.

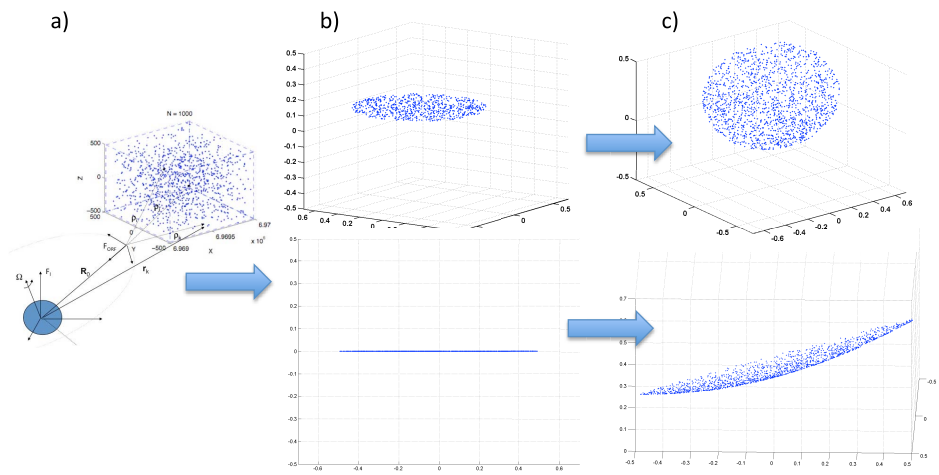

Figure 7. Re-shaping of a) amorphous cloud to b) disk and c) paraboloid.

6 Numerical results and discussion

The simulation results shown in Figure 7 were obtained by commanding the grains to conform to a prescribed optical surface. The cloud is first shaped into a disk, then into a paraboloid of specified focal length and diameter. The numerical results indicate that the force required to shape 1 meter diameter disk into parabola is of the order of 10^{-8} N. Assuming a grain shape which is asymmetric to incoming light, the torque required to align 1 micron grain is of the order of 10^{-15} Nm. For the computation time as a function of the number of grains N, preliminary results indicate an order $N^{1.43}$ scaling on a 8Gb, 1067 MHz RAM MacOSX computer with a 3.06 GHz Intel Core 2 Duo processor. With this metric, the same simulation for a system of N=1000 grains takes 5.4 hours, and 146 hours (i.e., 6 days) for a system with N=10,000 grains. Therefore, efficient ways to simulate this complex system, where not only the time scales of natural system dynamics, but also the sampling times of the Guidance, Navigation, and Control are included, remain to be fully explored. These methodologies would include GPU acceleration and multigrid solvers for the cloud dynamics, and will be the subject of future investigations [9], [20]. Figure 8 shows snapshots of the simulations of the entire imaging system with the cloud as an aperture.

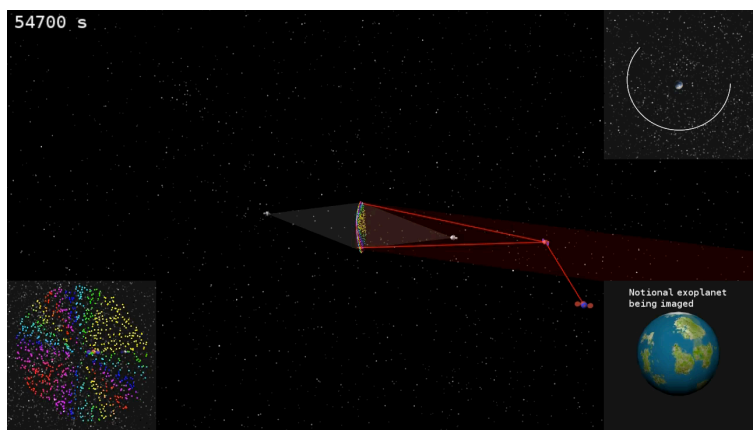

Figure 8. Snapshot of simulation.

Conclusions

In this paper, we have presented some ideas regarding the modeling, dynamics and control aspects of *granular spacecraft*. We have addressed the modeling and autonomous operation of a distributed assembly (the cloud) of large numbers of grains, controlled by opto-mechanical interactions. The modeling and simulation of a representative concept was also discussed. The application considered so far was a reflective imaging system for astrophysics, but many unexplored applications of granular spacecraft are yet to be discovered.

Acknowledgments

This research was carried out at the Jet Propulsion Laboratory, California Institute of Technology, under a contract with the National Aeronautic and Space Administration under the NASA Innovative Advanced Concepts Program.

References

[1] Ashkin, A.: Acceleration and trapping of particles by radiation pressure, Phys. Rev. Lett. **24**. 156-159, 1970.

[2] Axelrad, D.R.: Micromechanics of Solids, Elsevier Scientific Publishing Company, Amsterdam, 1978.

[3] Born, M., and Wolf, E.: *Principles of Optics*, 2nd edition, Pergamon Press, 1964, pp. 400.

[4] Brady, D.J., Hagen, N.: *Multiscale lens design*, Opt. Express 17, 10659-10674, 2009.

[5] Eringen ,C.: Microcontinuum Field Theories, Springer Verlag, 1999.

[6] Fuchs, N.A.: *The Mechanics of Aerosols*, Dover Publications, 1989.

[7] Gazi, V., and Passino, K.: Stability Analysis of Clouds, Proc. Of the American Control Conference, Anchorage, AK, May 8-10, 2002, pp. 1813-1818.

[8] Ghanem, R., and Spanos, P.: Stochastic Finite Elements, a Spectral Approach, Dover Publications, New York, 2003.

[9] Greengard, L.: The numerical solution of the N-body Problem, Computers in Physics, March-April 1990, pp. 142-152.

[10] Grzegorczyk, T., Kemp, B. A., Kong, J.A.: Trapping and binding of an arbitrary number of cylindrical particles in an in-plane electromagnetic field, J. Opt. Soc. Am. A, 23(9) Sept. 2006.

[11] Grzegorczyk, T., Kemp, B. A., Kong, J.A.: *Passive guiding and sorting of small particles with optical binding forces*, Opt. Lett., 31(22), Nov. 2006.

[12] Kadowaki, H., and Liu, W.K.: A Multiscale Approach for the Micropolar Continuum Model, Computer Modeling in Engineering and Science, 2005, vol.7, no. 3, pp. 269-282.

[13] Kokhanovsky. A. A.: *Cloud Optics*, Springer, 2006.

[14] Labeyrie, A.: Standing Wave and Pellicle: A Possible Approach to Very Large Space Telescopes, Astronomy and Atrophysics, 77, L1-L2, 1979.

[15] Lerman, K., Martinoli, A., Galstyan, A.: *A Review of Probabilistic Macroscopic Models for Swarm Robotic Systems*, in Swarm Robotics Workshop: State-of-the-art survey, edited by E. Sahin and W. Spears, LCNS 3342, Springer-Verlag, Berlin, 2005, pp.143-152.

[16] Mettler E., Breckenridge W.G., and Quadrelli M.B.: *Large Aperture Telescopes in Formation: Modeling, Metrology, and Control,* The Journal of the Astronautical Sciences, vol. 53, no.5 October-December 2005, pp.391-412.

[17] Mogilner, A., Edelstein-Keshet, L.: A Non-local Model for a Cloud, Journal of Mathematical Biology, 1999, no. 38, pp. 534-570.

[18] Molmud, P., "Expansion of a Rarefield Gas Cloud into a Vacuum," The Physics of fluids 3, 362-366 (1960).

[19] Palmer, A.J.: *Radiation-induced Orientation of Atmospheric Aerosols*, J. OP. Soc. America A, vol. 8, no. 2, February 1991.

[20] Pfalzner, S, and Gibbon, P.: Many-Body Tree Methods in Physics, Cambridge University Press, 1996.

[21] Reif, J.H., and Wang, H., Social Potential Fields: A Distributed Behavioral Control for Autonomous Robots, Robotics and Autonomous Systems 27 (1999) 171-194.

[22] Siljak, D.D.: Decentralized Control of Complex Systems, Academic Press, 1990.

[23] Van de Hulst, H. C.: *Light Scattering by Small Particles*, Dover Publications, 1981.